Rec...

NOV 2 8 1990

CONF-900923--6

"The submitted manuscript has been authored by a contractor of the U.S. Government under contract No. DE-AC05-84OR21400. Accordingly, the U.S. Government retains a nonexclusive, royalty-free license to publish or reproduce the published form of this contribution, or allow others to do so, for U.S. Government purposes."

CONF-900923--6

DE91 004398

Electron Ion Interactions in Crystal Channels: Collisions in Ultra-dense Electron Media

S. Datz, P.F. Dittner, J. Gomez del Campo,
H.F. Krause, T.M. Rosseel and C.R. Vane

Oak Ridge National Laboratory,
Oak Ridge, Tenessee 37831-6377 USA

Abstract

Dielectronic excitation of H-like S, Ca and Ti is shown to occur in the dense electron gas of a crystal channel. Cross sections for collisional ionization of the short lived excited states can then be determined. Ionic excitation can also be achieved by resonant coherent excitation in which case specific m states can be excited for further study.

Introduction

In recent years considerable progress has been made in the study of collisions of multiply charged ions with electrons. Areas which have been opened to investigation include excitation, ionization, radiative recombination and dielectronic recombination. All of these processes are contributors to the dynamics of hot plasmas. However, in high density plasmas collisions of short lived excited ionic states with electrons also play a significant role and, until now, have not been amenable to study. We have utilized the channeling effect to create conditions under which such processes may be studied.

Ions entering a crystal at small angles with respect to low order crystaline axes and planes are constrained in their motion and interact only with weakly bound conduction or valence electrons [1]. Thus ions passing through a channel with velocity $v_i \gg v_f$, the Fermi velocity of the conduction electrons, may be viewed a being bombarded with a flux of electrons with velocity $v_e \simeq v_i$ with a distribution of energies determined by the Fermi distribution of momenta for the electrons in the channel. These electrons can participate in the formation of excited states by either direct excitation or by recombination processes [2]. Then, because of the great electron density ($> 10^{23}/\mathrm{cm}^3$), in the channel they can participate in secondary electronic collisions which further excite or ionize the short lived excited species.

Specific excited states of ions in channels may also be prepared by the process of resonant coherent excitation [3, 4, 5]. Here the ion is excited by the periodic potential of the crystal lattice. As it passes a row of atoms with atomic spacing, d, it experiences a perturbation with frequency (v_i/d). Excitation from state i to state j can occur when $hK(v_i/d) = \Delta E_{ij}$ where K is a harmonic $= 1, 2, 3\ldots$. Ions excited in this manner may be prepared in specific m states and ionization of these species by electronic collisions in channels may also be studied.

Experimental

The experiments were carried out using the 25-MV tandem accelerator of the Holifield Heavy Ion Research Facility (HHIRF) at ORNL. Ion beams were colimated and passed through channels in thin crystals and measurements were made of *a)* the charge state distribution of the emergent ions using either electrostatic or magnetc deflection and a solid state position sensitive detector and, *b)* the X-ray spectra using a Si(Li) detector. In some cases coincidences between charge capture and X-ray emission were measured.

In fig. 1 we show a measure of the "frozen" charge state effect using 315 MeV Ti^{q+}(q = 20,21,22) beams passing through a $< 100 >$ channel in a 2.6 μm Si crystal and compare it to passage through the same crystal in a random direction. In the random direction, we obtain an equilibrium charge-state distribution independent of input charge state. For injection in the channeled direction, > 85% of the beam exits in its initial charge state.

The Si(Li) X-ray detector used had a resolution of 145 eV at 5.9 keV. For ions $Z \gtrsim 15$ we are easily able to resolve K-X rays from relaxation to a totally empty K shell from those arising from filling a K vacancy in an ion already containing a 1s electron. In fig. 2, we show X-ray spectra for 315 MeV Ti^{q+}(q = 20,21,22) channeled in $< 100 >$ Si (2.6 μm) taken in coincidence with electron capture, $q \rightarrow q-1$. The peak at 5.1 KeV corresponds to a $(2p1s) \rightarrow 1s^2$ transition. The peak at 5.3 KeV comes from a $2p \rightarrow 1s$ transition in the one electron ion.

* Presently visiting Tage Erlander Professor at Manne Siegbahn Institute of Physics, Frescativägen 24, S-104 05 STOCKHOLM, Sweden

MASTER

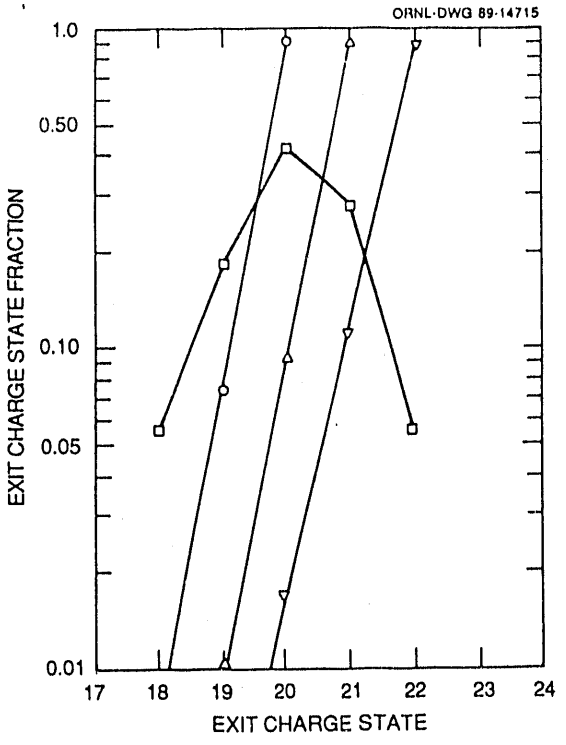

Fig. 1. Exit charge state distributions for injection of 315 MeV Ti^{20+} (o), Ti^{21+} (Δ), Ti^{22+} (∇) in a < 100 > channel in Si 2.6 μm thick, and ([ ]) exit charge distribution for random direction.

Radiative Electron Capture

The radiative electron capture (REC) peaks shown in fig. 2 arise from recombination of Fermi electrons (e_f) with the penetrating ions. In the case of the bare ion $e_f + Ti^{22+} \rightarrow Ti^{21+}(1s) + h\nu$ (fig. 2, part III) and for the one electron ion $e_f + Ti^{21+}(1s) \rightarrow Ti^{20+}(1s^2) + h\nu$ (fig. 2, part II). The shapes of the peaks are determined by the Compton profile of the electrons in the channel and fit very well with a 10 eV Fermi distribution. Moreover, since the Fermi width is determined by the electron density and the radiative recombination cross sections are accurately known, we have a measure for expected profile for resonant collisional excitation processes, the electron target thickness and hence the cross section for production of other X-rays in the spectrum.

Results and Discussion

Consider, for example, a hydrogen-like ion passing through a crystal channel at a velocity $v_i \gg v_f$, with a relative velocity corresponding to that required to excite a K electron and to simultaneously capture the exciting electron into an L shell. The formation of this doubly excited state is the exact reverse of a KLL Auger transition.

A summary of most of the reactions which could occur under these conditions is given below, in equation 1.

$$I.\quad A^{(Z-1)^+}(1s) + e \rightarrow \left[A^{(Z-2)^+}2\ell 2\ell'\right]^{**}.$$

$$II.\quad a)\ \left[A^{(Z-2)^+}(2\ell 2\ell')\right]^{**} \rightarrow A^{(Z-1)^+}(1s) + e$$

$$b)\ \left[A^{(Z-2)+}(2\ell 2\ell')\right]^{**} + e \rightarrow \left[A^{(Z-2)^+}(2\ell' 2\ell'')\right]^{**} + e.$$

$$III.\quad a)\ \left[A^{(Z-2)^+}(2\ell 2\ell')\right]^{**} \rightarrow \left[A^{(Z-2)^+}(1s2\ell)\right]^{*} + \underline{h\nu_1}$$

$$b)\ \left[A^{(Z-2)^+}(2\ell 2\ell')\right]^{**} + e \rightarrow \left[A^{(Z-2)^+}(2\ell 3\ell)\right]^{**} \xrightarrow{e} \left[A^{(Z-1)^+}(2\ell)\right]^{*} + 2e.$$

$$IV.\quad a)\ \left[A^{(Z-2)^+}(1s2\ell)\right]^{*} \rightarrow \underline{\left[A^{(Z-2)^+}(1s^2)\right]} + \underline{h\nu_2}$$

$$b)\ \left[A^{(Z-2)^+}(1s2\ell)\right]^{*} + e \rightarrow \left[A^{(Z-2)^+}(1s3\ell)\right]^{*} \xrightarrow{e} \left[A^{(Z-1)^+}(1s)\right] + 2e.$$

$$V.\quad a)\ \left[A^{(Z-1)^+}(2\ell)\right]^{*} \rightarrow \left[A^{(Z-1)^+}(1s)\right] + \underline{h\nu_3}$$

$$b)\ \left[A^{Z-1)^+}(2\ell)\right]^{*} + e \rightarrow \left[A^{(Z-1)^+}(3\ell)\right]^{*} \xrightarrow{e} \underline{A}^{Z+} + 2e.$$

Equation 1

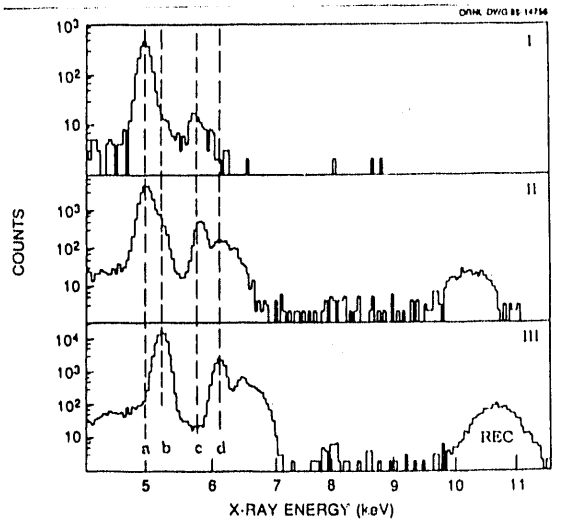

Fig. 2. X-ray spectra (singles) for 315 MeV Ti^{q+} channeled thorugh < 100 > Si 2.6 μm thick: (I) $q = 20$, (II) $q = 21$, and (III) $q = 22$ taken in coincidence with emergent charge state ($q - 1$). Specific features identified in the spectra are, respectively: (a) $1s2\ell \rightarrow 1s^2$, (b) $2p \rightarrow 1s$, (c) $1s3\ell \rightarrow 1s^2$, and (d) $3p \rightarrow 1s$. K-radiative electron capture X-rays appear at 10.3 KeV in II and 10.7 keV in III.

In a dilute electron target, only eqns 1-I, 1-III.a, and 1-IV.a are involved. The observable end products would be $h\nu_1$ from a $2\ell 2\ell' \rightarrow 1s2\ell$ transition and $h\nu_2$ from a $1s2\ell \rightarrow 1s^2$ transition and an ion of decreased charge $A^{(Z-2)^+}$ all in coincidence. However, in a dense medium when collisional rates become comparable to radiative rates, the other channels come into play. The collisional path leads to either $h\nu_3$ from a $2\ell \rightarrow 1s$ transition (eqn. I-V.a) or to complete ionization (eqn. I-V.b).

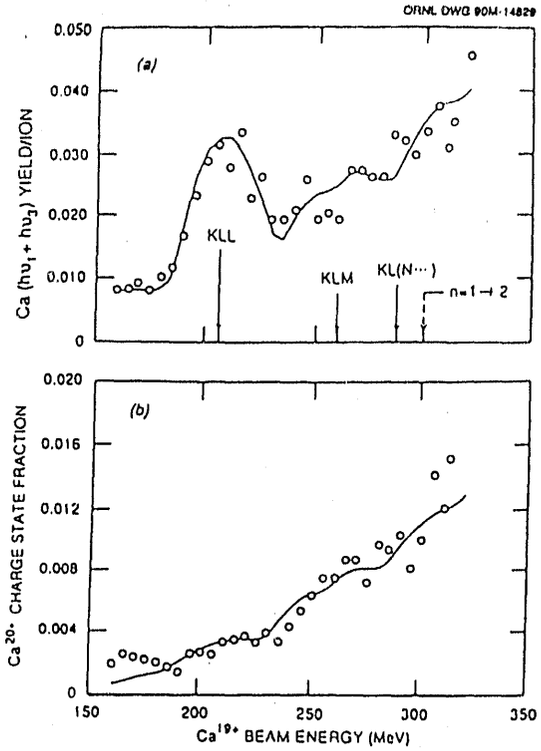

Fig. 3. (a) Yield of $h\nu_1(2\ell n\ell' \rightarrow 1sn\ell')$ plus $h\nu_3(2\ell \rightarrow 1s)$ calcium X-rays (see eqn. 1) and (b) charge fraction of Ca^{20+} ions as a function of Ca^{19+} ion energy incident on a < 100 > channel in Si (1.2 μm thick). The smooth curves are results of a computer simulation as described in the text.

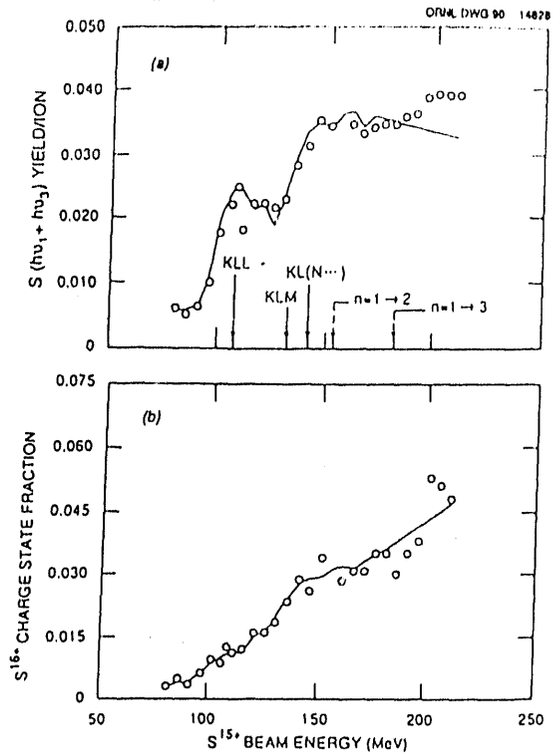

Fig. 4. (a) Yield of $h\nu_1(2\ell n\ell' \rightarrow 1sn\ell')$ plus $h\nu_3(2\ell \rightarrow 1s)$ sulphur X-rays (see eqn. 1) and (b) charge fraction of S^{16+} ions as a function of S^{15+} ion energy incident on a < 110 > channel in Si (1.2 μm thick). The smooth curves are results of a computer simulation as described in the text.

Magnitudes of these contributions can be estimated by assuming rapid collisional substate mixing [6], $n\ell \leftrightarrow n\ell'$ and then using the fastest available radiative and Auger rates. The radiative and Auger rates have been tabulated by Seely [7]. The ionization cross sections are estimated from the Lötz semi-empirical formula [8]. The excitation cross sections used are obtained from the Seaton formula [9].

No calculations exist for the cross sections for fine structure mixing (eqn. 1-II.b) for the ions in question. However, if we use the recent calculation [6] on, e.g., $(2s^2) \rightarrow (2s2p\ ^3P_2)$ transition in Fe^{22+} we obtain a cross section of $\sim 3 \times 10^{-16}$ cm^2 at a velocity corresponding to KLL excitation of Fe^{23+}. Since the fine structure splitting decreases with decreasing Z, the corresponding cross sections for the ions in question should be even higher. The main point is that these cross sections are so large that complete mixing is assured. We have no direct calculation for the dielectronic excitation cross section (i.e., eqn. 1-I) instead, we estimate it from measurements of RTE cross sections on the same or similar systems. The collisional rates, r_i, are obtained from

$$r_i = \sigma_i\ \rho_e\ v_i$$

where ρ_e is the electron density taken to be 1.44×10^{23} cm^{-3} for the Si < 110 > channel[10] and σ_i is the cross section for the considered process. However, since the dielectronic excitation process (eqn. 1-I) is a resonant one, the actual rate is grossly reduced (factor of ~ 1000) due to the Compton spread in relative energies. In our calculation, we use a 10 eV Fermi distribution for the electrons in a < 110 > Si channel. This value is taken from the work of Appleton et al. [10], and we derived a similar Fermi width from our measurement of the radiative electron capture (REC) peak (e.g., see fig. 2).

In fig. 3a, we show for channeled Ca^{19+} the yield per injected ion of $(h\nu_1 + h\nu_3)$ (eqn. 1-III.a and 1-V.a) as a function of ion energy. The features correspond to dielectronic excitation of KLL, KLM, KLN, etc., and, at 300 MeV, to direct $1s \rightarrow 2p$ excitation. The energies at which these contributions should appear are indicated by the arrows at the bottom of fig. 3a. The solid curves in fig. 3a are calculated from rate equations shown in eqn. 1, folded with the Compton profile of the 10 eV Fermi distribution. The populations of the ten lowest hydrogen- and helium-like configurations ($1s$ to 3ℓ and $1s^2$ to $3\ell 3\ell'$, respectively) are iteratively solved and summation bins for numbers of X-rays emitted are accumulated in 400 steps through the

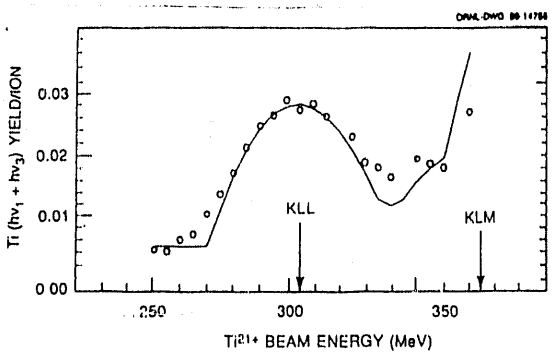

Fig. 5. (a) Yield of $h\nu_1(2\ell n\ell' \rightarrow 1sn\ell)$ plus $h\nu_3(2\ell \rightarrow 1s)$ titanium X-rays (see eqn. 1) as a function of Ti^{21+} ion energy incident on a < 110 > channel in Si (1.2 μm thick). The smooth curve is a result of a computer simulation as described in the text.

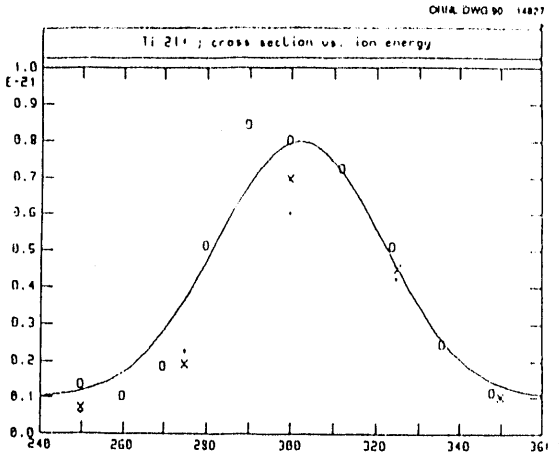

Fig. 6. Coincidence measurements for $Ti^{21+} + e \rightarrow Ti^{20+} + h\nu$ in < 110 > Si as a function of Ti ion energy. Yield in the KLL resonance region as a function of crystal thickness; 0–1.1 μm, + 2.1 μm, X 2.8 μm.

crystal length of 1.2 μm. charge-state fractions and x-ray yields per ion are calculated, including effects of Auger and X-ray decay of excited ions downstream of the crystal. It should be noted that the only normalization is the addition of backgrounds linear in projectile energy and that the predicted values are absolute in X-rays per ion. Using the same rate coefficients, we can calculate, e.g., the yield of Ca^{20+} ions (cf. eqn. 1-V.b) and plot it together with the experimental data in fig. 3b.

In the case of Ca^{19+}, the radiative processes dominate, e.g., the ratio of rates for the first branch point in eqn. 1 (III.a/III.b) $\simeq 5$. In the case of S^{15+}, the radiative rates are slower and the excitation and ionization cross sections are higher so that the collisional channel comes more into play, i.e., for S^{15+} (III.a/III.b) $\simeq 1$. In fig. 4a, we show, as a function of S^{15+} ion energy, the data for the yields of $(h\nu_1 + h\nu_3)$. In fig. 4b we show the S^{16+} charge fraction which is correspondingly higher than the totally stripped ion fraction for Ca. The solid curves are calculated in the same manner as for Ca^{19+} above.

In the case of Ti^{21+}, (III.a/III.b) $\cong 9$. Accordingly, the number of totally stripped ions becomes vanishingly small, but the effect is easily seen in the X-ray channel alone as demonstrated in fig. 5.

In all the above we have made many assumptions concerning rates. To validate these assumptions we take a simpler case where radiative processes should dominate (i.e. where secondary electron collisions are unimportant) and see whether we can derive a cross section for dielectronic recombination. For this we chose the case of the KLL resonance in Ti^{21+} and measured the X-ray spectra in coincidence with Ti^{20+}. This measures the dielectronic recombination rate. The importance of secondary collisions can be measured by varying the thickness of the Si crystal used i.e. in the absence of secondary collisions the yield will be linearly proportional to thickness. The results for the yield per unit thickness is shown for the three thicknesses used 1.1, 2.1, and 2.8 μm in fig. 6 and are sensibly independent of thickness. The curve in fig. 6 is for a 10 eV Fermi distribution fit to the points. From this we can derive a cross section of $0.70 \pm 0.10 \times 10^{-21}$ cm^2 per electron. To compare with RTE data [11] (where the width of the resonance is determined by the Compton profile of H_2) we multiply our values by 1.2 and, since the RTE cross sections are given per molecule, we divide those values by two. The value thus obtained is 0.72 ± 0.12.

Resonant Coherent Excitation

In previous work [1, 3, 4, 5] we showed that hydrogenic ions passing through axial and planar channels could be excited from $n = 1$ to $n = 2$ when the frequency of perturbation by the atoms in the crystal spaced a distance d apart came into resonance when the spacing between eigenstates i and j,

$$\Delta E_{ij} = hK(v_i/d)$$

where K is a harmonic 1,2,3 ... of the (v_i/d) frequency. We also showed that the degeneracy in the $n = 2$ levels is removed; first by the assymetry in the crystal field and second by Stark mixing of $2s$ with $2p_z$ (z being the direction of ionic motion) which is caused by the wake field following the ion. The main point in the context of this paper is that the resonant frequency, and hence velocity, for excitation to $2p_{x,y}$ is different than that for $2p_z$ and they can be excited selectively.

In our previous work we used C, N, O and F ions available at EN Tandem energies. These light ions when excited to $n = 2$ had a high probability of ionizing by secondary collision in the channel (cf. eq. 1) and the resonances were observed as an increase in the population of totally stripped ions.

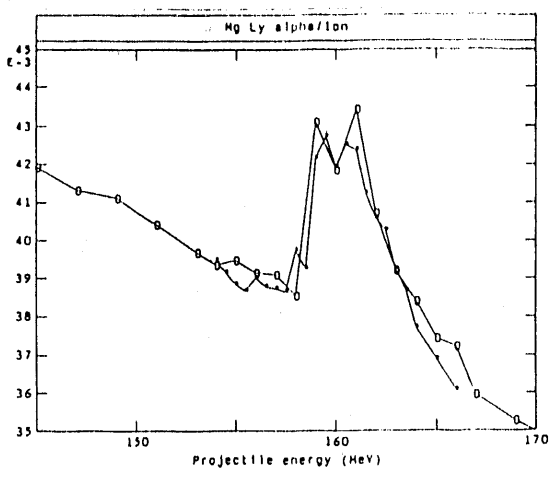

Fig. 7. Resonant coherent excitation of Mg^{11+} (4th harmonic) in < 100 > Au observed as Mg Ly α emission; Yield of X-rays as a function of Mg^{11+} energy.

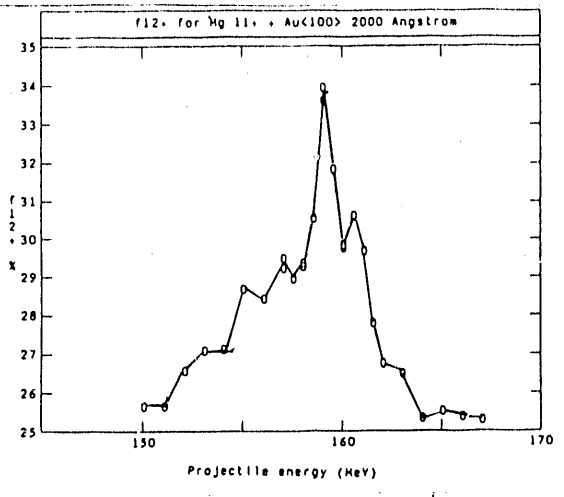

Fig. 8. Resonant coherent excitation of Mg^{11+} (4th harmonic) in < 100 > Au observed by increase in ionization; charge fraction of Mg^{12+} as a function of Mg^{11+} energy.

In the present work [12] we report preliminary results on a higher Z ion, Mg^{11+}, where the $n = 2$ ionization cross section is small enough to permit escape of some of the excited ions from the crystal with the subsequent emission of radiation. Since we can excite different orientations (m states) of the ion selectively by varying the velocity we can measure the separate ionization cross sections for these states by determining the yields of totally stripped ions compared to those which emit a Ly α X-ray.

We used the HHIRF to supply beams of Mg^{11+} at energies from 145 to 170 MeV. These were passed through an Au crystal 1200 Å thick in the < 100 > directions (d = 4.08 Å). The emergent ion charge distribution and two Mg K X-ray yields were measured as a function of ion energy. The results are shown in figs 7 and 8. The fourth harmonic of the $n = 1$ to 2 resonance ($\Delta E_{ij} = 1468$ eV) should appear at 163 MeV if the transition were to occur in vacuum. The crystal field effects shift the peaks to lower energies. The upper of the two peaks corresponds to excitation into a $2p_z$ state and the lower to a $2p_x$ or $2p_y$ state. A comparison of the two curves shows that the probability of escape from the crystal without ionization (X-ray cyrve) is greater for ions in the $2p_z$ state than those in the $2p_{x,y}$ state.

At this point these RCE data are not yet quantified and are presented as proof of principal for experiments which measure electron bombardment ionization cross sections for short lived excited states with specific polarization.

This research was sponsored by the U.S. Department of Energy, Office of Basic Energy Sciences, Division of Chemical Sciences, under Contract No. DE-AC05-840R21400 with Martin Marietta Energy Systems, Inc.

References

1. Datz, S., and Moak, C.D.: "Heavy-Ion Channeling," in Treatise on Heavy-Ion Science, ed. Bromley, D.A., Vol. **6**, Astrophysics, Chemistry, and Condensed Matter, Chapter 5 (1985) pp. 169–240.

2. Datz, S., Vane, C.R., Dittner, P.F., Giese, J.P., Gomez del Campo, J., Jones, N.C., Krause, H.F., Miller, P.D., Schulz, M., Schöne, H., and Rosseel, T.M.: Phys. Rev. Lett. **63**, 742 (1989); Nucl. Inst. Meth. **B48**, 114 (1990).

3. Datz, S., Moak, C.D., Crawford, O.H., Krause, H.F., Dittner, P.F.. Gomez del Campo, J., Biggerstaff, J.A., Miller, P.D., Hvelplund, P., and Knudsen, H.: Phys. Rev. Lett. **40**, 843 (1979).

4. Datz, S., Moak, C.D., Crawford, O.H., Krause, H.F., Miller, P.D., Dittner, P.F., Gomez del Campo, J., Biggerstaff, J.A., Knudsen, H., and Hvelplund, P.: Nucl. Inst. Meth. **170**, 18 (1980).

5. Miller, P.D., Krause, H.F., Biggerstaff, J.A., Crawford, O.H., Datz, S., Dittner, P.F., Gomez del Campo, J., Moak, C.D., Neskovic, N., Pepmiller, P.L., and Brown, M.D.: Nucl. Inst. Meth. **B13**, 56 (1986).

6. Kim, Y.-K., and Desclaux, J.-P.: Phys. Rev. **A38**, 1805 (1988).

7. Seely, F.: Atomic Data and Nuclear Data Tables **26**, 137 (1981).

8. Lötz, W.: Z. Physik **206**, 206 (1968).

9. Seaton, M.J.: "The Theory of Excitation and Ionization by Electron Impact," in Atomic and Molecular Processes, ed. Bates, D.R., p. 374, New York, Academic Press 1962.

10. Appleton, B.R., Ritchie, R.H., Biggerstaff, J.A., Noggle, T.S., Datz, S., Moak, C.D., Verbeck, H., and Neelavathi, V.N.: Phys. Rev. **B19**, 4347, see discussion on page 4356, (1979).

11. Presently no direct RTE measurement exists for H-like Ti^{21+}. To obtain a value for comparison we take the results for Li-like $Ti^{19+} + H_2$ given by Reusch et al. (Nucl. Inst. Meth. **B23**, 137 (1987)) and scale to Ti^{21+} using the values for Li-like, He-like and H-like Ca given by Tannis et al. (Phys. Rev. **A34**, 2543 (1986).

12. Collaborating on this part of the work were Iwata, I., Komaki, M., Kimura, K., and Yamazaki, Y., University of Tokyo and Honda, F., and Fujimoto, F., University of Osaka.

END

DATE FILMED

12 / 10 / 90